Preparation of Y_2O_3:Yb,Er Infrared-to-Visible Conversion Phosphor Fine Particles Using an Emulsion Liquid Membrane System

Takayuki Hirai,* Takuya Orikoshi, and Isao Komasawa

Department of Chemical Science and Engineering, Graduate School of Engineering Science, and Research Center for Solar Energy Chemistry, Osaka University, Toyonaka, Osaka 560-8531, Japan

Received February 22, 2002. Revised Manuscript Received June 10, 2002

Upconverting phosphor fine particles (Y_2O_3:Yb,Er) have been prepared, using an emulsion liquid membrane (ELM, water-in-oil-in-water (W/O/W) emulsion) system, consisting of Span 83 (sorbitan sesquioleate) as the surfactant and VA-10 (2-methyl-2-ethylheptanoic acid), DTMBPA (bis(1,1,3,3-tetramethylbutyl)phosphinic acid), or Cyanex272 (bis(2,4,4-trimethylpenthyl)phosphinic acid) as the extractant (cation carrier). The Y, Yb, and Er ions were extracted, from the external water phase, and stripped into the internal water phase, to make precursor composite oxalate particles. The precursor particles obtained in the VA-10 system were mainly 20−60 nm in size, together with a smaller amount of submicron-sized spherical particle, and were much smaller than those prepared in homogeneous aqueous solution (1−10 μm in size). The molar composition of the particles, $\{M/(Y+Yb+Er)\}_p$ (M = Yb or Er), prepared in the VA-10 and DTMBPA systems, was almost proportional to that of the feed external solution, $\{M/(Y+Yb+Er)\}_f$. Calcination of the composite Y−Yb−Er oxalate particles obtained in the VA-10 system produced Y_2O_3:Yb,Er particles about 50 nm in size. The aggregation of the oxide primary particles was found to be suppressed by increasing the surfactant concentration in the VA-10 system. The Y_2O_3:Yb,Er particles demonstrated an upconversion emission at 662 nm, by infrared excitation (λ_{ex} = 960 nm). At an external feed aqueous solution of $\{Yb/(Y+Yb+Er)\}_f = 0.08$, $\{Er/(Y+Yb+Er)\}_f = 0.01$, the 662 nm emission peak intensity reached a maximum value. The present upconverting phosphor fine particles, about 50 nm in diameter, may be applied to the reporters in immunoassays or DNA assays.

Introduction

An emulsion liquid membrane (ELM, water-in-oil-in-water (W/O/W) emulsion) system has been studied for the separation of metals, in which the metal ions are extracted, from the external water phase, into the organic membrane phase, where they are then stripped and concentrated into the internal water phase. Recently, it has been found that the internal water phase is capable of being used for the preparation of size-controlled and morphology-controlled fine particles,[1] since the micrometer-sized internal water droplet has a restricted reaction area. In addition to the formation of several single-component fine particles,[1−3] the preparation of composite particles, such as acicular ferrite particles,[4] and Y_2O_3:Eu phosphor fine particles[5] has also been reported, using the ELM system.

Luminescent reporter materials form an excellent alternative to radioisotopes and are increasingly used in immunoassays. At present, luminescence assays generally provide high sensitivity and the simultaneous use of multiple fluorophores with different spectral characteristics (multiplexing). Nevertheless, greater sensitivity improved multiplexing, and performance under extreme test conditions is continuously demanded.

There has been a growing interest in upconverting phosphor compounds, that emit visible or ultraviolet radiation, when excited with infrared light. The upconversion process produces emitted photons with a higher energy than the excitation photon energy and arises when two or more absorbed photons, of low energy (IR), cause the emission of a single photon of visible light through radiative energy transfer. Such materials are composed typically of trivalent rare-earth absorbing (e.g. Yb, Er, and Sm) and emitting (e.g. Er, Ho, Pr, and Tm) ions, acting in a multiphoton process.[6] Figure 1 shows the basic mechanism for a two-photon upconversion process. Upconverting phosphors have a number of properties that are advantageous for use in

* To whom correspondence should be addressed. Telephone: +81-6-6850-6272. Fax: +81-6-6850-6273. E-mail: hirai@cheng.es.osaka-u.ac.jp.

(1) Majima, H.; Hirato, T.; Awakura, Y.; Hibi, T. *Metall. Trans. B* **1991**, *22B*, 397−404.
(2) Hirai, T.; Okamoto, N.; Komasawa, I. *J. Chem. Eng. Jpn.* **1998**, *31*, 474−477.
(3) Hirai, T.; Okamoto, N.; Komasawa, I. *Langmuir* **1998**, *14*, 6648−6653.
(4) Hirai, T.; Kobayashi, J.; Komasawa, I. *Langmuir* **1999**, *15*, 6291−6298.
(5) Hirai, T.; Hirano, T.; Komasawa, I. *J. Mater. Chem.* **2000**, *10*, 2306−2310.
(6) Auzel, F. E. *Proc. IEEE* **1973**, *61*, 758−786.

10.1021/cm0202207 CCC: $22.00
Published on Web 07/20/2002

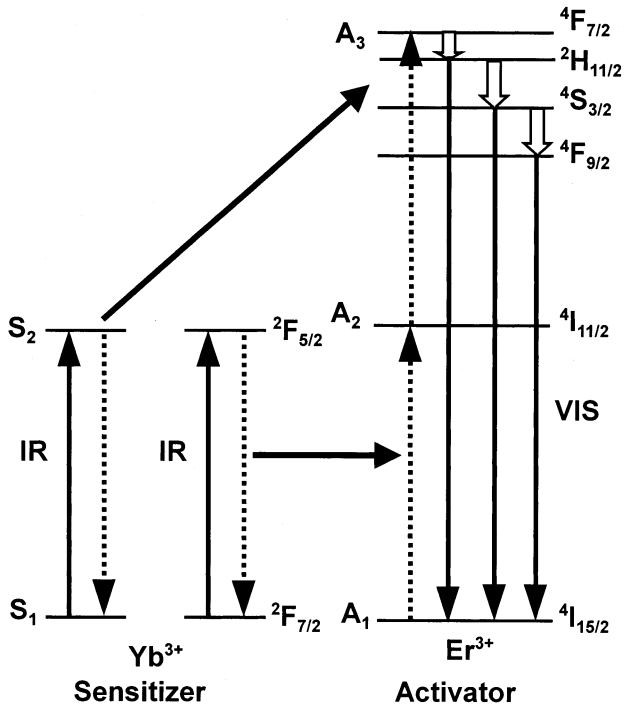

Figure 1. Mechanism of a two-photon upconversion process.

the *in vitro* assay of biological compounds.[7,8] Because the upconversion process is unique in nature, there is a complete lack of any background phosphorescence from the assay biochemistry, when using upconverting phosphors. The optical properties of the phosphors are also completely unaffected by their environment (e.g. buffer chemistry and assay temperature), since the upconversion process occurs solely within the host crystal. Excitation is performed using infrared laser diodes, which are compact, have high power, and are also inexpensive. The upconversion emission bands from the lanthanide ions are narrow, which is also advantageous for multiplexed assays. There has been a growing development of a class of nonisotopic detection labels by coupling upconverting phosphors to biological compounds. In this design, nanometer-sized upconverting phosphors are detected through upconversion emission and the attached biological compounds recognize specific analytes, such as protein, DNA, or viruses. These nanoconjugates are biocompatible and are suitable for use in immunoassays and DNA assays. When combined with sandwich immunoassay, the use of nanometer-sized upconverting phosphor probes should open new possibilities in detecting native biological compounds.

In previous studies, the heavier rare-earth (Dy, Y, and Yb) oxalate particles of submicrometer size were prepared with ELM systems, containing 2-methyl-2-ethylheptanoic acid (VA-10)[2,5] or bis(1,1,3,3-tetramethylbutyl)-phosphinic acid (DTMBPA)[3,5] as the extractant (cation carrier). Ultrafine particles of 20−60 nm diameter were obtained in the VA-10 system, while spherical oxalate particles 200−600 nm in diameter were obtained using the DTMBPA system. The present work has been carried out to prepare ultrafine upconverting phosphor particles. Composite Y−Yb−Er oxalate fine particles were prepared in the ELM systems, by feeding Yb and Er ions into the external water phase together with Y ions. ELM systems containing VA-10, DTMBPA, or Cyanex272 as cation carrier were also employed. The composite Y−Yb−Er oxalate particles prepared in the ELM system were calcined to obtain upconverting phosphor, Y_2O_3:Yb,Er, and the size, morphology, and upconversion emission of the composite oxide particles were then investigated, as compared to those of the particles prepared in the homogeneous aqueous solution.

Experimental Section

2-Methyl-2-ethylheptanoic acid (VA-10), supplied by Shell Chemical Co., was used as the extractant, and sorbitan sesquioleate (Span 83, supplied by Tokyo Kasei Kogyo Co., Ltd., Tokyo) was used as the surfactant. DTMBPA (bis(1,1,3,3-tetramethylbutyl)phosphinic acid) was supplied by Nippon Chemical Industrial Co. Ltd., Tokyo. Cyanex272 (bis(2,4,4-trimethylpenthyl)phosphinic acid) was supplied by Mitsui Cytex, Ltd. Yttrium nitrate ($Y(NO_3)_3$), ytterbium nitrate ($Yb(NO_3)_3$), erbium nitrate ($Er(NO_3)_3$), oxalic acid, sodium acetate, ethylene glycol, and acetone were supplied by Wako Pure Chemical Industries, Ltd.

The oxalate particles were prepared via a procedure similar to that reported previously.[2,3,5] The internal water phase for the emulsion (0.1 mol/L oxalic acid) and the organic membrane phase (kerosene containing 0.5 mol/L extractant with differing quantities of Span 83) were mixed at a volume ratio of 1:1 (O/A ratio = 1) and emulsified by means of a mechanical homogenizer (12 000 rpm). The concentration of Span 83 was 5 wt % in the majority of cases, but was also varied in the range 3−7 wt % as required. The mean diameter of the internal water droplets produced was ~3 μm. The resulting W/O emulsion (10 mL) was then added to the external water phase (50 mL of $Y(NO_3)_3$, $Yb(NO_3)_3$, and $Er(NO_3)_3$ aqueous solution) and stirred vigorously, with a magnetic stirrer, to form the W/O/W emulsion.

The total metal concentration of the external aqueous solution was always fixed at 4 mmol/L, but the molar composition of the feed external solution, $\{Yb/(Y+Yb+Er)\}_f$ and $\{Er/(Y+Yb+Er)\}_f$, was varied. CH_3COONa (0.02 mol/L) was added to the external solution for those cases, using VA-10, to maintain the external water phase pH greater than a value of 4. The size of the emulsion drops, dispersed in the external water phase, was less than 2 mm. After stirring for the required time, the W/O emulsion was then separated from the external aqueous solution and demulsified by adding ca. 50 mL of ethylene glycol or acetone. The particles, formed in the water droplets, were then separated by centrifuge, washed with acetone, and dried in vacuo. The oxalate particles were finally calcined in air, at 1073 K for 2 h, to obtain the oxide particles, Y_2O_3:Yb,Er.

Both the composite oxalate and the composite oxide particles were characterized by scanning electron microscopy (SEM, Hitachi S-5000 or S-2250N), powder X-ray diffraction (XRD, Philips PW-3050), and thermogravimetric/differential thermal analysis (TG-DTA, Shimadzu TG-DTA50). To determine particle composition, the particles were dissolved in 1 mol/L HCl and the metal concentrations measured, using an inductively coupled argon plasma atomic emission spectrometer (ICP-AES, Nippon Jarrell-Ash ICAP-575 Mark II). To determine the metal concentrations in each phase of the ELM system, the separated W/O emulsion was first demulsified electrically and the organic membrane phase was then stripped with 1 mol/L HCl. The metal concentrations both in the resulting stripping solution and in the external water solution were determined by ICP-AES. The metal concentration in the internal water phase was then calculated by mass balance. A near-infrared laser diode (λ_{ex} = 960 nm, NAMUTEC NT-2000LT) was used as the excitation source. The measurement of the upconversion emission spectra of the particles was carried out using a

(7) Niedbala, R. S.; Vail, T. L.; Feindt, H.; Li, S.; Burton, J. L. *Proc. SPIE* **2000**, *3913*, 193−203.
(8) Hampl, J.; Hall, M.; Mufti, N. A.; Yao, Y. M.; MacQeen, D. B.; Wright, W. H.; Cooper, D. E. *Anal. Biochem.* **2001**, *288*, 176−187.

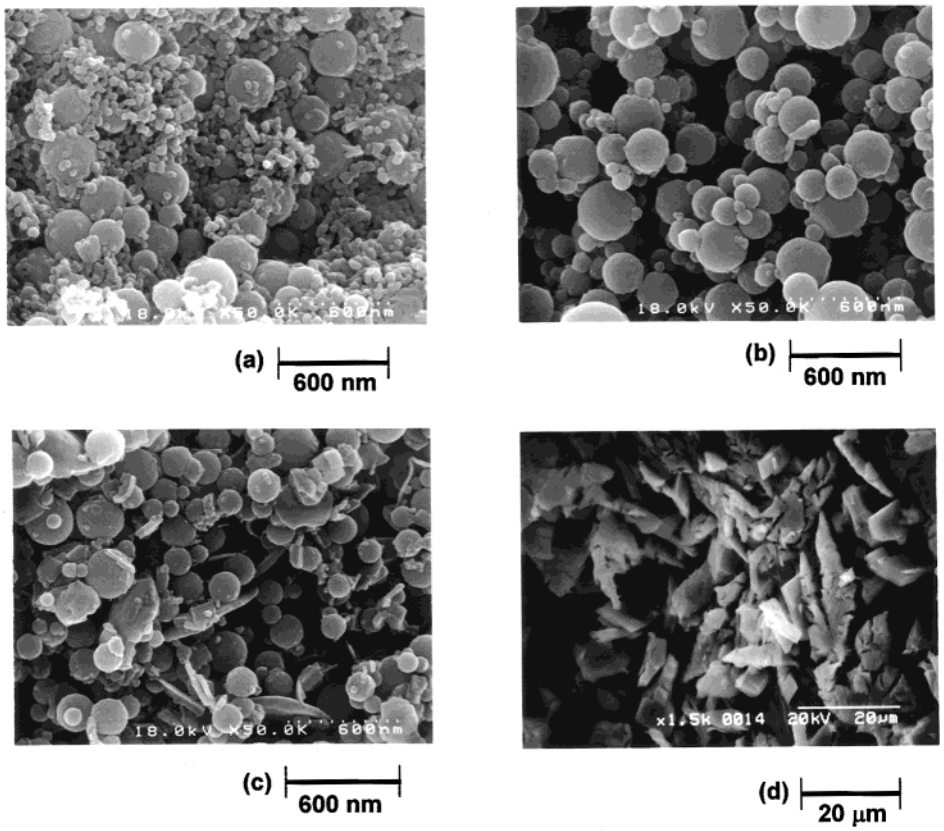

Figure 2. SEM images for composite Y−Yb−Er oxalate particles, prepared at $\{Yb/(Y+Yb+Er)\}_f = \{Er/(Y+Yb+Er)\}_f = 0.05$ in the (a) VA-10, (b) DTMBPA, and (c) Cyanex272 systems, under the Span 83 concentration 5 wt %, and in (d) homogeneous aqueous solution.

spectrofluorometer (JASCO FP-777) with a solid sample holder (JASCO FP-1060). The sizes of the particles obtained were measured with a laser scattering particle-size distribution analyzer (Horiba LA-910W).

Results and Discussion

Size and Morphology of the Composite Oxalate Particles. Typical SEM images of composite oxalate particles, obtained at a value of $\{Yb/(Y+Yb+Er)\}_f = \{Er/(Y+Yb+Er)\}_f = 0.05$ in the VA-10, DTMBPA, and Cyanex272 systems are shown in Figure 2. Mainly 20−60 nm ultrafine particles were obtained, in the VA-10 system, together with a smaller amount of submicron-sized spherical aggregates (Figure 2a), whereas better well-defined spherical particles, ranging from 60 to 400 nm in diameter, were obtained using the DTMBPA system (Figure 2b). The particles prepared, in the Cyanex272 system, were mainly spherical, of about 200 nm in diameter, but were formed together with smaller flat or elongated particles ∼30−100 nm in diameter (Figure 2c).

The size and morphology of the composite particles obtained in the VA-10 and DTMBPA systems are similar to those obtained in the respective ELM systems, for the yttrium oxalate particles[2,3] and the composite Y−Eu oxalate particles.[5] The SEM images for composite particles obtained, in the homogeneous aqueous solution, by adding a 0.01 mol/L rare-earth nitrate solution ($\{Yb/(Y+Yb+Er)\}_f = \{Er/(Y+Yb+Er)\}_f = 0.05$) to a 0.1 mol/L oxalic acid solution, are shown in Figure 2d for comparison. In this case, the composite particles are greater than 1 μm in size, are nonspherical, and exhibit flat or elongated features. In comparison to the homogeneous system, the ELM system is therefore much more effective in controlling both the size and the morphology of the particles, because of the isolated nature of the precipitation in each internal water droplet.

Composition of the Composite Oxalate Particles. Figure 3 shows the time-course variations for the mole percent compositions of the three ions, in the external water phase, in the organic membrane phase, and in the internal water phase, for all the extractant systems, where the following conditions $\{Yb/(Y+Yb+Er)\}_f = \{Er/(Y+Yb+Er)\}_f = 0.1$ apply. In the VA-10 system (Figure 3a), it is seen that the transport of both the Yb and Er ions into the internal water phase is completed within a time of 30 min. The results also show that appreciable amounts of the metal ions are not accumulated within the membrane phase, thus indicating that the ions are stripped effectively into the internal water phase, by the oxalic acid. The extractability for the Y ions by VA-10 is lower than that for Yb and Er ions.

In the DTMBPA system (Figure 3b), the Y and Er ions are extracted rather slowly, although the transport of Yb into the internal water phase is completed within 20 min. The percentage retention of metal ions, within the organic membrane phase, is about 20% for all three ions.

In the Cyanex272 system (Figure 3c), the transport of all three ions into the internal water phase is completed within 60 min. The percent extraction obtained for Yb ions is about 70%, but this is less than those of Y and Er ions, which lie at about 90%.

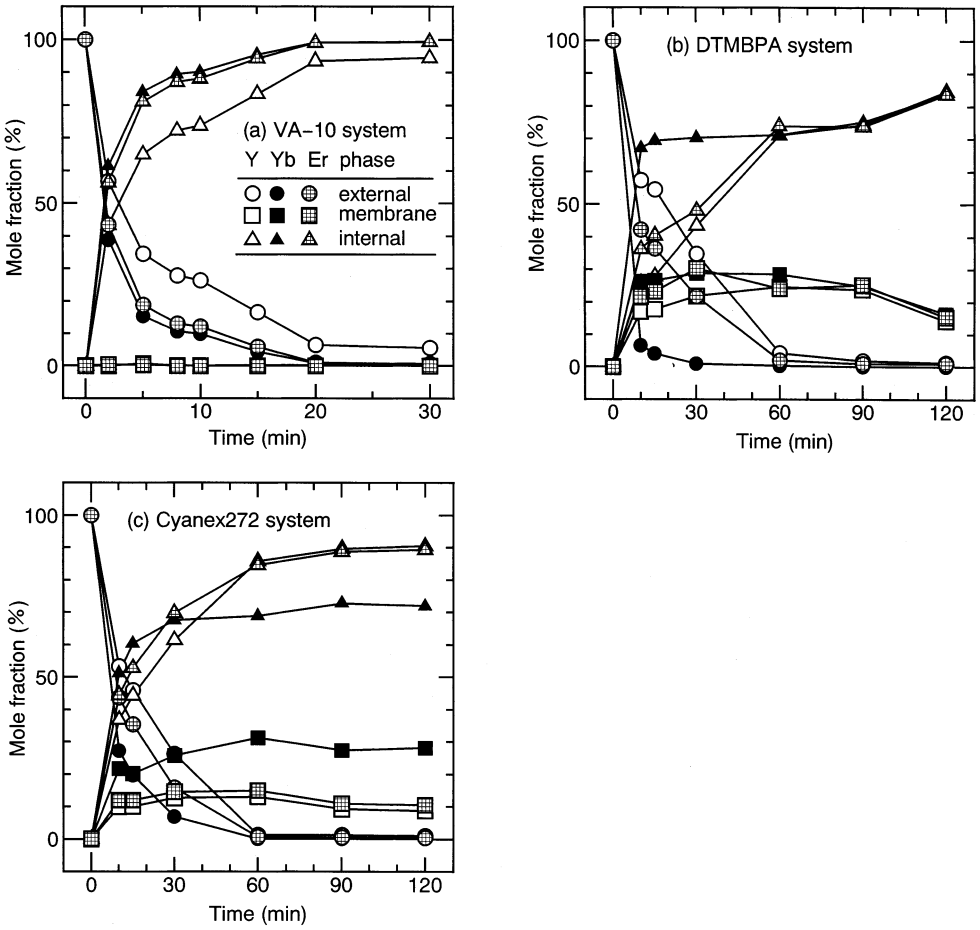

Figure 3. Time-course variations for the mole fraction composition of Y, Yb, and Er ions in the external water phase, organic membrane phase, and internal water phase in the (a) VA-10, (b) DTMBPA, and (c) Cyanex272 systems at $\{Yb/(Y+Yb+Er)\}_f = \{Er/(Y+Yb+Er)\}_f = 0.1$. The mole fraction in the initial external water phase is set as 100%.

Figure 4 shows plots, for all systems, of the molar composition for the particles, $\{M/(Y+Yb+Er)\}_p$ (M = Yb or Er), versus that of the feed external solution, $\{M/(Y+Yb+Er)\}_f$. For composite oxalate particles, prepared in the homogeneous system, it was found that $\{M/(Y+Yb+Er)\}_p$ is almost identical to $\{M/(Y+Yb+Er)\}_f$. This result indicates that there is therefore no difference in the precipitation rate obtained. In the VA-10 and DTMBPA systems, $\{M/(Y+Yb+Er)\}_p$ is also almost identical to $\{M/(Y+Yb+Er)\}_f$, despite the differences in the transportation rate for all three ions, into the internal water phase. Thus, in the case of the VA-10 and DTMBPA systems, the molar composition of the particles can be controlled by changing the composition of the feed external solution. For the Cyanex272 system, the $\{Yb/(Y+Yb+Er)\}_p$ value is greater than $\{Yb/(Y+Yb+Er)\}_f$, though fewer Yb ions were stripped into the internal water phase, as compared to the amounts of Y and Er ions.

Calcination of the Composite Oxalate Particles. Figure 5 shows the TG-DTA curves for the oxalate particles prepared in the VA-10 system, which resemble those obtained for the particles prepared in the homogeneous system. The particles exhibit three steps in the oxalate TG curve, which occur respectively at about 373, 573, and 773 K. Endothermic peaks (at 357, 590, and 852 K) in the DTA curve accompany these weight loss steps. They correspond to formation of the dehydrated oxalate, the dioxycarbonate, and the oxide. Particles, prepared according to the VA-10 and to the homogeneous systems, were calcined at 1073 K for 2 h and were characterized by XRD, as shown in Figure 6. XRD measurement of the thermal decomposition products of the oxalate particles showed that both types of oxalate particle decomposed completely to form their corresponding oxide. The thermal behavior indicates the formation of dehydrated oxalate, dioxycarbonate, and finally corresponding oxide. Similar characteristic XRD patterns for Y_2O_3:Yb,Er were obtained for particles prepared in the DTMBPA and Cyanex272 systems. Figure 7 shows SEM images for the oxide particles prepared both in the homogeneous and in the ELM systems, following calcination at 1073 K for 2 h. Calcination of the oxalate particles, prepared in the VA-10 system, produces oxide particles about 50 nm in size, such as those shown in Figure 7a. Calcination of particles, prepared in the DTMBPA and Cyanex272 systems, brings about some contraction of the particles, probably caused by the elimination of both H_2O and CO_2. At 1073 K the surface of the particles becomes roughened, producing a particle size of less than 300 nm, as shown in Figure 7b and c. Calcination of the particles, prepared in the homogeneous system, results in some contraction of the particles, with a product 1−10 μm in size, as shown in Figure 7d.

Control of the Aggregation for the Composite Oxide Primary Particles. In the previous study, the aggregation of rare-earth oxalate primary particles in

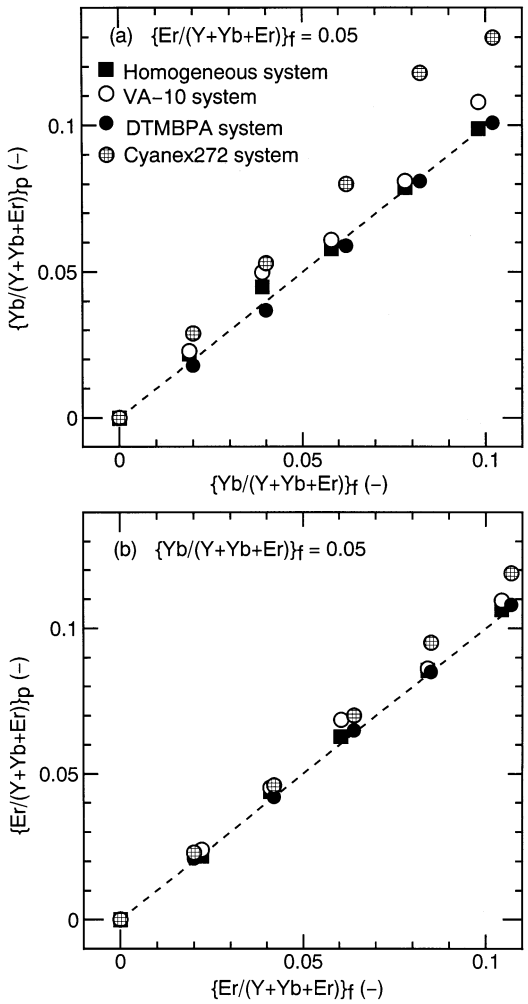

Figure 4. Relationship between the feed molar ratio, $\{M/(Y+Yb+Er)\}_f$, (M = Yb or Er) and the composition of the particles, $\{M/(Y+Yb+Er)\}_p$, for the particles in the ELM and homogeneous systems at (a) $\{Er/(Y+Yb+Er)\}_f = 0.05$ and (b) $\{Yb/(Y+Yb+Er)\}_f = 0.05$.

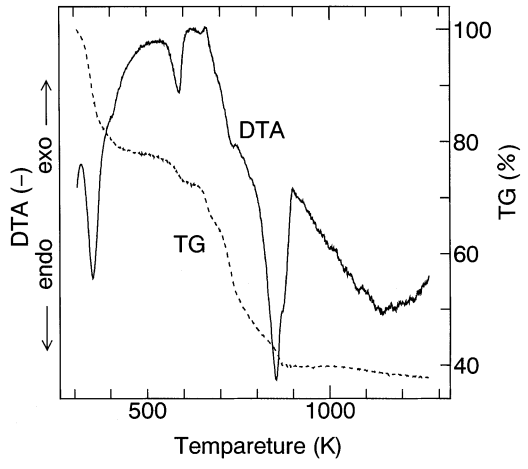

Figure 5. TG-DTA curves for composite Y−Yb−Er oxalate particles, prepared in the VA-10 system at $\{Yb/(Y+Yb+Er)\}_f = \{Er/(Y+Yb+Er)\}_f = 0.05$.

the VA-10 system was found to depend on the surfactant concentration.[2] Composite oxalate particles were therefore prepared in the VA-10 system, with differing Span 83 concentrations (3−7 wt %), and these were calcined at 1073 K for 2 h. The amount of the spherical aggregates seems to decrease, with increasing Span 83 concentration up to 7 wt %, as may be judged by a comparison of the SEM images (Figure 8b with 7 wt % Span 83, and Figure 7a with 5 wt %). Thus, control of aggregation of the primary particles is shown to be feasible, according to the VA-10 system.

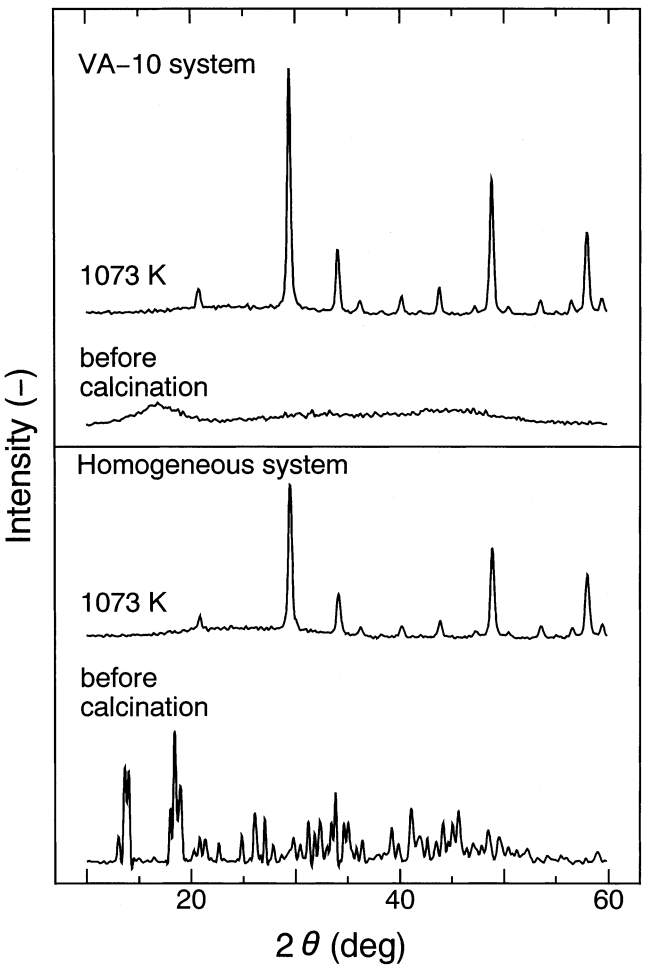

Figure 6. X-ray diffraction patterns for composite Y−Yb−Er oxalate particles, prepared at $\{Yb/(Y+Yb+Er)\}_f = \{Er/(Y+Yb+Er)\}_f = 0.05$ in the VA-10 and homogeneous systems, before and following calcination (oxide) for 2 h at 1073 K.

A possible interpretation of these results is that there may be some interaction between the oxalate primary particles and the extractant/surfactant at the organic membrane phase/internal water phase interface. A stronger interaction in the VA-10 system may thus prevent the oxalate primary particles from aggregating within the internal water droplets.

Luminescent Properties of the Composite Oxide Particles. The first photon of infrared light (960 nm) elevated an electron to the $^2F_{5/2}$ level of Yb^{3+}, and the ion may then decay radiatively from this excited state back to the ground state ($^2F_{7/2}$). Alternatively, it can transfer the energy to the Er^{3+} ion. This energy can promote an electron from $^4I_{15/2}$ to the $^4I_{11/2}$ state, and if the latter is already populated, a transition from the $^4I_{11/2}$ to the $^4F_{7/2}$ state can occur. Figure 9 shows typical upconverting emission spectra from Y_2O_3:Yb,Er particles prepared both in the ELM and in the homogeneous systems. The peaks were assigned to the following transitions: green emission in the 520−580 nm region was assigned to the $(^2H_{11/2}, {}^4S_{3/2}) \rightarrow {}^4I_{15/2}$ transition, and

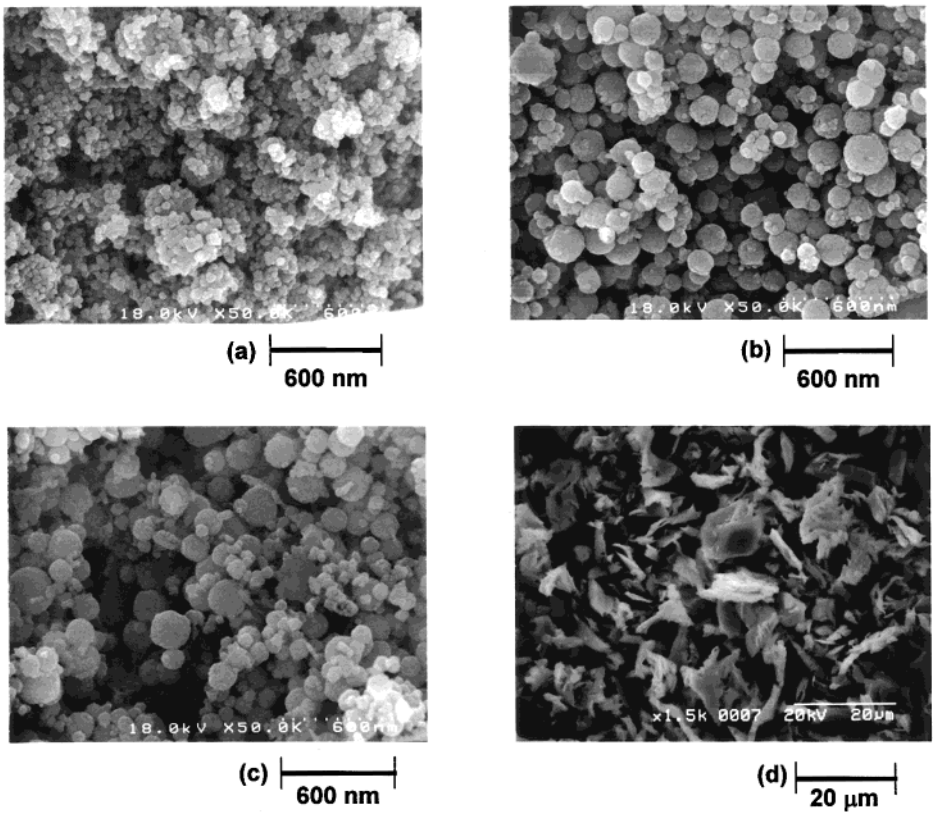

Figure 7. SEM images for Y_2O_3:Yb,Er particles, obtained by calcination of composite Y−Yb−Er oxalate particles prepared in the (a) VA-10, (b) DTMBPA, (c) Cyanex272, and (d) homogeneous systems at $\{Yb/(Y+Yb+Er)\}_f = \{Er/(Y+Yb+Er)\}_f = 0.05$. Calcination temperature: 1073 K.

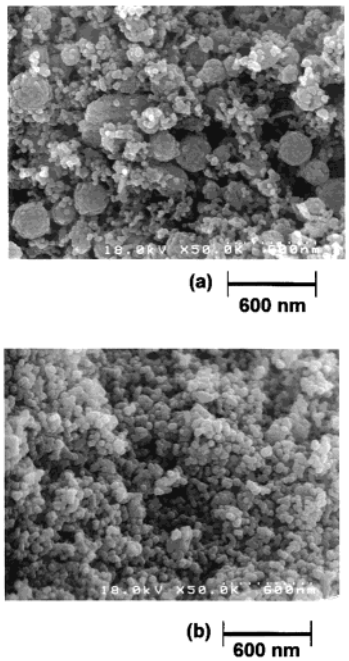

Figure 8. SEM images for Y_2O_3:Yb,Er prepared at $\{Yb/(Y+Yb+Er)\}_f = \{Er/(Y+Yb+Er)\}_f = 0.05$ in the VA-10 system, under the surfactant concentrations (a) 3 wt % and (b) 7 wt % and calcination for 2 h at 1073 K.

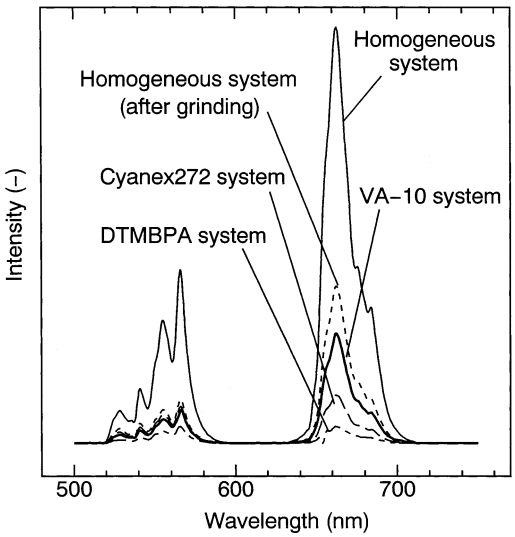

Figure 9. Upconversion emission spectra from Y_2O_3:Yb,Er particles prepared at $\{Yb/(Y+Yb+Er)\}_f = \{Er/(Y+Yb+Er)\}_f = 0.05$, formed in the ELM and homogeneous systems, calcined for 2 h at 1073 K. $\lambda_{ex} = 960$ nm.

red emission in the 650−700 nm region was assigned to the $^4F_{9/2} \rightarrow {}^4I_{15/2}$ transition for Er^{3+} ions. The main emission peak, obtained at 662 nm, corresponds to a red emission. The effective absence of the green component in the Er emission is attributed to several ion-pair energy transfer processes, bypassing the green-emitting states in exciting the red-emitting ones and tending to depopulate the green-emitting states very rapidly.[9]

Particles prepared in the VA-10 system show higher emission intensities than those for the DTMBPA and Cyanex272 systems, though the particle sizes in the VA-10 system are much smaller than those for DTMBPA and Cyanex272. The observed difference in the trans-

(9) Wittke, J. P.; Ladany, I.; Yocom, P. N. *J. Appl. Phys.* **1972**, *43*, 595−600.

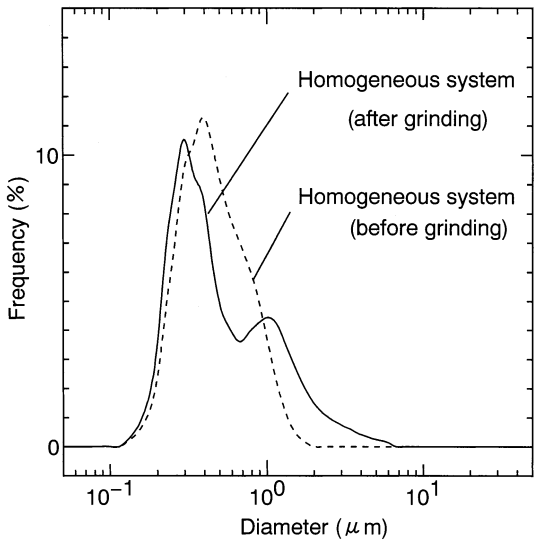

Figure 10. Size distribution for Y_2O_3:Yb,Er particles, obtained by calcination of composite Y−Yb−Er oxalate particles, prepared at $\{Yb/(Y+Yb+Er)\}_f = \{Er/(Y+Yb+Er)\}_f = 0.05$, formed in the homogeneous system. Calcination temperature: 1073 K.

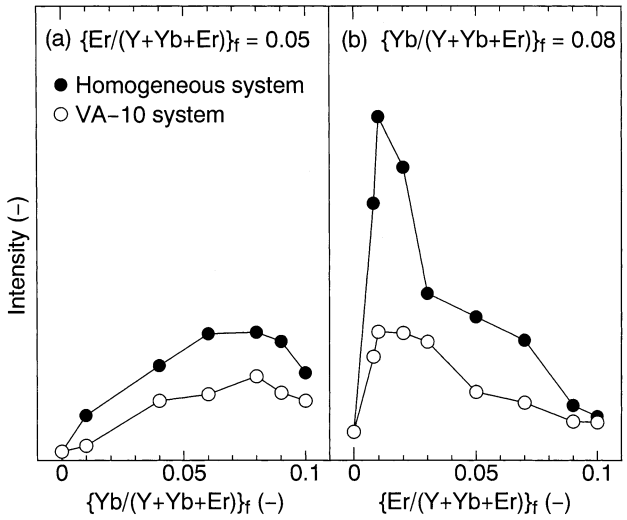

Figure 11. Variation of the 662 nm emission peak intensity from Y_2O_3:Yb,Er particles prepared at various (a) $\{Yb/(Y+Yb+Er)\}_f$ and (b) $\{Er/(Y+Yb+Er)\}_f$ values in the VA-10 and homogeneous systems. $\lambda_{ex} = 960$ nm.

portation rate for the rare-earth ions, into the internal water phase, may result in a heterogeneous distribution for the Yb and Er ions in particles prepared by the DTMBPA and Cyanex272 systems. The smaller particles, prepared in the ELM systems, demonstrated lower upconverting emission intensities than the larger particles, prepared in the homogeneous system. Surface defects have often been blamed for the decreasing emission intensities. This may become apparent with decreasing particle size and increasing surface area. It was found in the previous study[5] that the emission intensities from the larger Y_2O_3:Eu particles, prepared in the homogeneous system, are greater than those from the smaller particles, prepared in the ELM systems. When the larger particle materials were ground, using an agate mortar to narrow the size distribution, the emission intensities from the resulting particles were found to be decreased to a level comparable to those found for particles prepared in the ELM systems. As shown in Figure 10, the present particles, when prepared in the homogeneous system, show a wide size distribution, having two peaks at 0.3 and 1.0 μm. On grinding the particles in the agate mortar, the larger peak was reduced to a mean particle diameter of 0.4 μm, as shown in Figure 10. This value, however, is much greater than that as prepared in the ELM systems, although the emission intensity is remarkably decreased by grinding, as again indicated in Figure 9.

In the upconversion process, the 662 nm emission peak intensity may be affected by the dopant ion concentration. To test this, Figure 11a shows the variation of the peak intensity for the composite oxide particles, prepared in both the VA-10 and homogeneous systems, as a feed function of Yb, $\{Yb/(Y+Yb+Er)\}_f$. The emission intensity is seen to increase slowly from a value of $\{Yb/(Y+Yb+Er)\}_f = 0$, to attain a maximum at $\{Yb/(Y+Yb+Er)\}_f = 0.08$, after which it then decreases slowly. The sensitization effect of the Yb ion on the Er activator ion, thus, varies with the Yb ion concentration. The Yb_n aggregate ions ($n > 1$) formed, at higher concentrations, may act as trapping centers and thus dissipate the adsorbed energy nonradiatively, instead of transferring it to an Er activator ion. Figure 11b shows the variation in the emission peak intensity with respect to varying Er ion concentration, indicating that the emission peak intensity increases rapidly from the starting value of $\{Er/(Y+Yb+Er)\}_f = 0$, to reach a maximum at $\{Er/(Y+Yb+Er)\}_f = 0.01$ and then to decrease with a further increase of the concentration of Er. This behavior may be due to cross-relaxation or to energy migration to quenching centers where the excitation energy is lost nonradiatively. The migration occurs by energy transfer between activator ions. The quenching sites may be impurities or defects, which inevitably are present within the lattice.

Conclusion

Upconverting phosphor fine particles (Y_2O_3:Yb,Er) have been prepared using an emulsion liquid membrane (ELM, W/O/W emulsion) system, consisting of Span 83 (sorbitan sesquioleate) as surfactant and VA-10 (2-methyl-2-ethylheptanoic acid), DTMBPA (bis(1,1,3,3-tetramethylbutyl)phosphinic acid), and Cyanex272 (bis-(2,4,4-trimethylpenthyl)phosphinic acid) as alternative cation carriors. Precursor composite oxalate particles, obtained in the VA-10 system, are mainly 20−60 nm in size, together with a smaller amount of submicron-sized spherical particles, and are much smaller than those prepared in the homogeneous aqueous solution. The composition of the particles, $\{M/(Y+Yb+Er)\}_p$ (M = Yb or Er), can be controlled by the composition of the external feed aqueous solution, $\{M/(Y+Yb+Er)\}_f$, in the VA-10 and DTMBPA systems. Calcination of the composite oxalate particles, obtained in the VA-10 system, easily gives Y_2O_3:Yb,Er particles about 50 nm in size. In the VA-10 system, the aggregation of the primary particles is suppressed by increasing the surfactant concentration. The Y_2O_3:Yb,Er upconverting phosphor particles obtained by calcination of the composite particles showed an upconversion emission at 662 nm. At the conditions of an external feed aqueous solution to $\{Yb/(Y+Yb+Er)\}_f = 0.08$, $\{Er/(Y+Yb+Er)\}_f = 0.01$, the

662 nm emission peak intensity reaches a maximum. Upconversion phosphor fine particles, about 50 nm in diameter, may be applied to the luminescent reporter material for the detection of the targeted analyte in immunoassays or DNA assays.

Acknowledgment. The authors are grateful to Mr. Masao Kawashima of the Gas-Hydrate Analyzing System (GHAS) of Osaka University for his experimental assistance in the characterization of the particles and to the Division of Chemical Engineering for the Lend-Lease Laboratory Systems. The authors are also grateful for the financial support, through the Grant-in-Aid for Scientific Research (No. 13650813), from the Ministry of Education, Culture, Sports, Science, and Technology, Japan.

CM0202207